J. Phys. Res. Edu., Vol. 1, March 2024

A method of estimating the EAS cores of Monte Carlo showers for the GRAPES-3 experiment

Animesh Basak*

Department of Physics, University of North Bengal, Siliguri, WB, 734 013, India

The procedure of estimating the different extensive air shower (EAS) parameters is inherently linked to the accurate estimation of the cosmic-ray EAS cores. In EAS data analyses, the core of an EAS is estimated simultaneously with other crucial EAS parameters like shower size, shower age, etc. by fitting the lateral density data (LDD) of either the EAS charged secondaries or purely electrons with some suitably chosen lateral density function employing the maximum likelihood method. The present analysis estimates EAS cores using the LDD of electrons that fall on the scattered array detectors from the simulated EASs initiated by proton and iron primaries. Considering a densely packed detector array, including configurations akin to GRAPES-3, the research employs a straightforward weight average method (WAM) for the EAS core estimation. The findings reveal that around 95.5% of simulated showers exhibit EAS cores within a deviation range of approximately 1 m to 3 m from the actual cores of the CORSIKA Monte Carlo showers initiated by proton and iron primaries.

I. INTRODUCTION

Cosmic rays (CRs) are the high-energy particles originating from sources beyond our solar system, continually bombard the Earth's atmosphere. When these CRs collide with atmospheric nuclei, they trigger a cascade of secondary particles, resulting in what is known as an extensive air shower (EAS). Formation of an EAS is a complex phenomenon involving the interaction of CRs with the atmosphere, producing a myriad of secondary particles, including electrons, positrons, muons, photons, and hadrons. These particles propagate through the atmosphere, creating a shower-like pattern extending several square kilometers. One remarkable aspect of EASs is their immense energy. Primary CRs can possess energies ranging from 10^9 to 10^{20} eV, far surpassing the energies achievable in particle accelerators on Earth. As the primary CR particle collides with atmospheric nuclei, its energy is distributed among the secondary particles, leading to the development of the EAS. The study of EASs provides valuable insights into the properties and origins of primary CRs and the fundamental processes governing high-energy particle interactions in the cosmos. By analyzing the characteristics of air showers, crucial information about EASs can be inferred, such as the energy spectrum, composition, and arrival directions of CRs, shedding light on their astrophysical sources and acceleration mechanisms. Statistically, EASs exhibit a power-law distribution in terms of their energy spectrum, with

higher-energy events being less frequent than lower-energy ones. Some interesting characteristics of the distribution, like - the knee, the ankle and the GZK cutoff of the primary particle energy spectrum, reflect the underlying physics of CR interactions and are a vital feature analyzed by researchers to understand the nature of CR accelerators and the mechanisms responsible for their acceleration to such extreme energies. Furthermore, the statistical properties of EASs, including their lateral spread, lateral/radial particle density, and the depth of shower maximum development in the atmosphere, offer valuable constraints for theoretical models and simulations of CR propagation and interaction processes.

Detecting and analyzing EASs require sophisticated instruments and experimental setups, such as those employed in facilities like the GRAPES-3 experiment [1, 2]. The precision of measurements pertaining to EAS parameters rests upon the meticulous estimation of the EAS shower cores. Various methodologies are being explored to attain a more accurate core estimation. In the case of densely configured EAS arrays like GRAPES-3, employing the stated weighted average method (WAM) [3] through simulation is anticipated to streamline the proceedure while ensuring accuracy in delineating the EAS core.

The plan of the paper is as follows. A brief description of the GRAPES-3 experiment is given in Section II. The air shower simulations for the study is presented in Section III. Section IV describes briefly the EAS core estimation formulae. In Section V, the main results of the work with the necessary discussion is given. The paper ends with a conclusion in Section VI.

II. THE GRAPES-3 EXPERIMENTAL CONDITIONS

The GRAPES-3 (Gamma Ray Astronomy at PeV EnergieS; phase-3) [2] experiment is located in the mountain valley of Ooty, Tamil Nadu in southern India (11.4^o N, 76.7^o E, 2200 m a.s.l.). The air shower detector-array of the GRAPES-3 facility is a sprawling network of detectors designed to capture the cascades of secondary particles generated when CRs interact with the Earth's atmosphere. These detectors are deployed in a symmetric hexagonal geometry with different (X_i , Y_i , Z_i ; for i^{th} detector) coordinates. The meticulously designed EAS array consisting of 395 scintillators [1], each 1 m^2 in area with inter-detector separation of only 8 m (Fig. 1). The second major component of the GRAPES-3 experiment is the 560 m^2 GRAPES-3 muon detector that contains 16 tracking modules (each 35 m^2 in area and energy threshold of 1 GeV for vertical muons) [2], which provides reliable measurement of the muon size (Fig. 1).

FIG. 1: The GRAPES-3 detector array with a varying elevation, showing muon detectors module in the left and data acquisition center in the middle of the figure. The figure on the right represents the schematic layout of the detector array.

III. EAS SIMULATION

The simulation of EAS events involves a coupling between two distinct hadronic interaction models within the CORSIKA Monte Carlo (MC) program version 7.690 framework [4]. Specifically, the high-energy regime (above 80 GeV/n) is governed by the QGSJet 01 version 1c model [5], while the UrQMD model [6] characterizes the lower energy section (below 80 GeV/n). For the electromagnetic component, the EGS4 program library is employed. The EAS events are simulated to mirror the geographical location of the GRAPES-3 experiment. The kinetic energy thresholds for muons and electrons are set at 0.3 and 0.003 GeV. About 20000 showers are simulated for each of the proton and iron primaries, spanning primary energy ranges between 8×10^{14} eV and 3×10^{15} eV, with zenith angles constrained below 25°. In addition to this comprehensive data set, a numerous number of additional showers are simulated for each mentioned primary type, encompassing various specific primary energy values and zenith angles in order to broaden our quest.

IV. ESTIMATION OF THE EAS CORE

By default, CORSIKA simulates the core of each EAS at the centre of the detector plane (0,0). However, in reality, EAS cores are randomly distributed across the detector array. To reflect this reality in our shower simulations, we deliberately employ random numbers to distribute the EAS cores arbitrarily within the red hexagon [1] (refer to Fig. 1), which closely mimics the real-world scenarios. These cores are represented by coordinates (x_r, y_r). Subsequently, the core position of each shower is estimated as (x_e, y_e) by calculating the weighted mean of the first nineteen selected detectors with the highest-density of electron counts (ρ_i)

$$(x_e, y_e) = (\frac{\sum X_i \rho_i^2}{\sum \rho_i^2}, \frac{\sum Y_i \rho_i^2}{\sum \rho_i^2}); i = 1, ..19. \quad (1)$$

The core position of each shower is estimated considering *plane detector* configuration (i.e. taking $Z_i = 0$ for each detector) as well as for *actual detector* configuration (i.e. taking $Z_i \neq 0$ and the modified coordinate of each detector for varying elevation is $(X_i^Z, Y_i^Z) = (X_i + Z_i \tan\Theta \cos\phi, Y_i + Z_i \tan\Theta \sin\phi)$, where ϕ is the polar angle of detector plane, and Θ is the zenith angle of an EAS).

The error in the core estimation is determined as follows:

$$\Delta r = \sqrt{(x_r - x_e)^2 + (y_r - y_e)^2}. \quad (2)$$

V. RESULTS AND DISCUSSIONS

The WAM estimates the EAS core quite accurately for hexagonal symmetric density distribution for the detector configuration of the GRAPES-3 experiment centre. Here, hexagonal symmetric density distribution represents a scenario for the energy deposition of an EAS in the detector array in such a manner that there is a highest density detector surrounded by six next highest-density detectors inside the first ring, which are surrounded by twelve next highest-density detectors inside the second ring, and the weighted average of these nineteen density detectors represents the estimated core of the EAS. The CR showers with higher zenith angle and lower primary energy inhibit the hexagonal symmetric distribution of density of EAS electrons, thereby reducing the accuracy of the estimated core.

The primary challenges encountered in employing the WAM for the core analysis dwell around fluctuations in densities observed at the detectors, and the considerable spacing between them. Remarkably, these separations pose a significant issue with low-energy EASs, where the number of active detectors is minimal. An extensive hindrance of hexagonal symmetry in density distribution can be observed in Fig. 2 for EASs initiated by the proton with energy 10^{14} eV, and the problem rises with increasing zenith angle, thereby worsening the difficulty in estimating the EAS cores. Additionally, the highest density detectors are dispersed in such a manner that EASs exhibit multiple core structures, rendering the WAM ineffective in accurately pinpointing core locations using the mentioned nineteen highest density detectors particularly for inclined EASs initiated by low-energy primaries.

To mitigate the impact of density fluctuations, especially at lower energies, we adopted a cluster-based approach. In this method, we select the highest-density detector within a designated cluster for each shower event. Subsequently, the remaining eighteen detectors are chosen within a 25 m radial distance from this maximum density detector. The core location is then estimated utilizing the WAM, based on these chosen

nineteen highest density detectors. Through this approach, we find that for low-energy proton showers ($4 \times 10^{12}\text{eV} \leq E \leq 1 \times 10^{13}\text{eV}$), we can accurately estimate the core location for 95% of events with an uncertainty of ± 5 m. In the energy range ($3 \times 10^{14}\text{eV} \leq E \leq 7.5 \times 10^{14}\text{eV}$), we found 95% events within ± 4 m for the actual detector array. The value of Δr (in m) within which 95.5% of events are present for p and Fe initiated showers, considering actual array configuration at two different average energies (0.3 PeV and 0.5 PeV) is shown in the Table I.

TABLE I: Δr (in m) for 95.5% events considering actual detector array

PCR	Proton		Iron	
$E(PeV)$	0.3	0.5	0.3	0.5
$\Theta = 0^o$	2.27	1.58	4.52	3.47
5^o	2.32	1.88	4.62	3.67
15^o	2.67	2.27	4.62	3.57
25^o	2.97	2.62	4.67	4.32

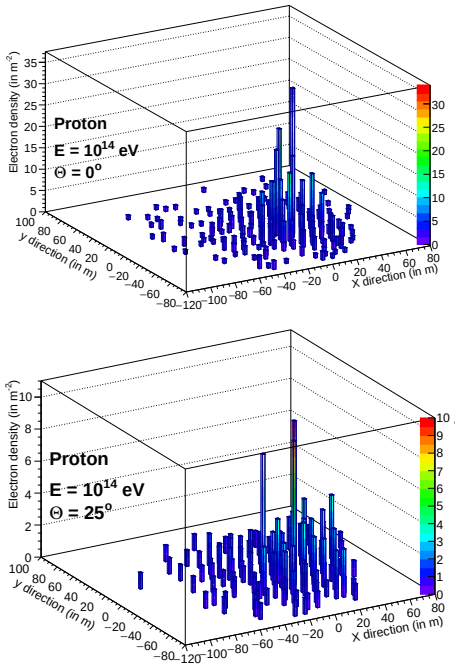

FIG. 2: Density plot for proton-initiated showers with E = 10^{14} eV and $\Theta = 0^o$ (*top*), and $\Theta = 25^o$(*bottom*).

The density fluctuations around the estimated core is minimal for high-energy showers, as illustrated in Fig. 3. Additionally, there is a noticeable contrast in density between the highest-density detector and other detectors registering hits. The cases involving high-energy showers, the strategic expansion of the cluster boundary is undertaken to envelop the whole of the detector array. This deliberate extension ensures

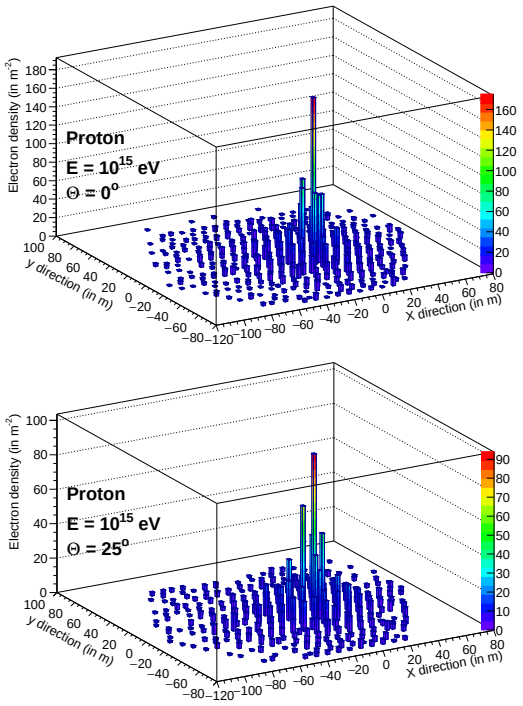

FIG. 3: Density plot for proton showers with E = 10^{15} eV and $\Theta = 0^o$ (*top*), and $\Theta = 25^o$(*bottom*).

the comprehensive selection of the 19 detectors exhibiting the highest-density. By broadening the scope of the cluster boundary to encapsulate the entire detector array, we guarantee the inclusive selection of these critical detectors, thereby focussing the pivotal attributes of the high energy shower event. Table II presents the Δr values (in m), which delineates the radial distance within which 95.5% of events occur for both p- and Fe-initiated showers. This analysis is conducted for both the plane detector array and the actual array, accounting for a geometric correction for the z-coordinate of each detectors. The Δr values are computed at three distinct average energies.

Finally, the methodology is applied to a data set comprising the entire 20000 showers initiated by each of proton and iron primaries, with primary energies falling within proximity to the knee region (8×10^{14}eV $-$ 3×10^{15}eV) and Θ not exceeding 25°. Illustrated in Fig. 4 is the population distribution of Δr for both proton and iron showers, considering the plane detector configuration of the GRAPES-3 array. Notably, the mean of this distribution stands at 0.074 m for proton and 1.094 m for iron showers. Conversely, when accounting for the actual detector configuration of the GRAPES-3 array, the mean values of the population distribution of Δr escalate to 1.094 m for proton and 1.385 m for iron showers as illustrated in Fig. 5.

TABLE II: Δr (in m) for different conditions.

PCR		Proton			Iron		
$E(PeV)$		0.8	1	3	0.8	1	3
Plane array (Δr)	$\Theta = 0^o$	1.33	1.23	1.08	2.42	1.93	1.08
	5^o	1.33	1.28	1.18	2.52	1.93	1.13
	15^o	1.58	1.33	1.28	2.72	2.82	1.28
	25^o	1.83	1.48	1.28	3.72	3.77	1.58
Actual array (Δr)	0^o	1.33	1.38	1.18	2.62	2.23	1.28
	5^o	1.43	1.38	1.23	2.57	2.32	1.28
	15^o	2.47	2.32	1.83	3.87	3.02	2.13
	25^o	3.82	3.48	3.32	4.87	4.12	3.57

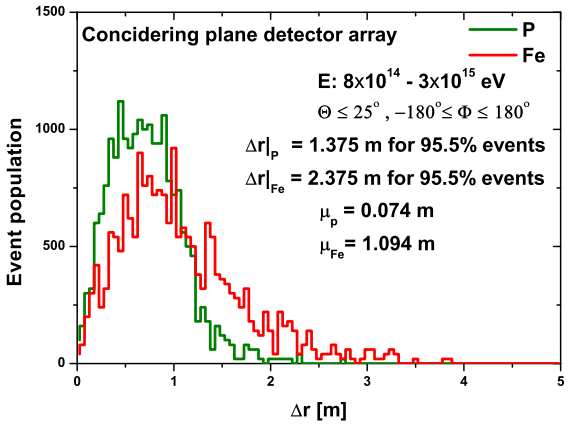

FIG. 4: Frequency distribution of Δr for the EASs produced by proton and iron primaries while considering plane array configuration of detectors.

VI. CONCLUSION

The analysis explored a methodology for accurately estimating the cores of EASs for a detector array like the GRAPES-3 experiment. We observed that the WAM proves effective, particularly in scenarios of high-energy showers with dense detector arrays. Initially, we encountered issues with density fluctuations and asymmetric density distributions over the whole detector array, prompting the exploration of novel approaches, such as cluster-based methods, to improve core estimation accuracy, especially in low-energy showers. As the energy of the primary particle increases, EASs exhibit larger shower sizes accompanied by an expanded lateral spread in density distribution, encompassing the entire configuration of the detector

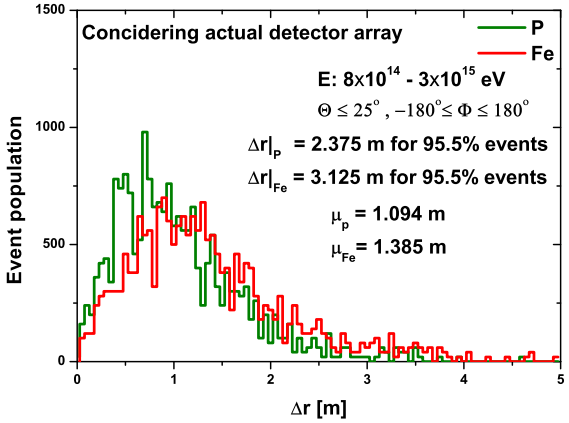

FIG. 5: Frequency distribution of Δr for the EASs produced by proton and iron primaries while considering actual array configuration of detectors.

array. Consequently, the cluster boundary is widened to encompass the entirety of the detector array, ensuring comprehensive coverage of the shower event. Notably, our findings emphasized the significance of geometric considerations and detector array configurations to accurately estimating the EAS core, which is crucial for reconstructing the showers and asociated EAS parameters.

Our investigation has used MC data generated by the CORSIKA code of version 7.690. It has been observed that the value of Δr is larger for an iron shower compared to a proton shower The iron nuclei have a larger interaction cross-section compared to protons. Consequently, the iron nuclei are more likely to interact with atmospheric particles, leading to more frequent collisions and interactions. Due to their intense atmospheric interactions, iron nuclei lose energy more rapidly as they travel through the atmosphere. The higher mass and energy of iron nuclei result in more energetic collisions with atmospheric particles, leading to a more significant number of secondary particle production. Consequently, the larger number of secondary particles in iron-initiated showers contributes to a higher attenuation effect as they propagate through the atmosphere. Protons, being lighter particles, tend to interact less frequently and penetrate deeper into the atmosphere before initiating the showering process compared to heavier nuclei like iron. These factors are responsible for smaller shower sizes for iron EASs than proton-initiated showers. Again, lower-energy primaries initiate fewer interactions and consequently produce fewer secondary particles, reducing shower size. The EASs with reduced shower sizes result in a sparser distribution of detector hits. This reduced the density of detectors due to EAS particles which may lead to more significant uncertainty in determining the precise location of the shower core, as fewer data points may be available for analysis.

The asymmetric lateral density distribution observed in the detector array for inclined extensive air showers primarily emanates from the unequal attenuation of secondary cosmic ray particles for different polar

angles in the shower front plane while propagating through the atmosphere, causing an unequal dispersion of secondary particles. Moreover, asymmetries in particle generation, atmospheric absorption, scattering processes, and the Earth's geomagnetic field together contribute to this asymmetry, resulting in enhanced uncertainty in EAS core estimation.

ACKNOWLEDGMENTS

A. Basak wants to express his sincere gratitude to Dr. R. K. Dey and Dr. A. Bhadra for their invaluable support and guidance throughout preparing this paper. Their expertise, encouragement, and constructive feedback have been instrumental in shaping the quality and direction of this research.

* Electronic address: animesh21@nbu.ac.in

[1] S. K. Gupta, *et al*, Nuclear Phys. B **196**, 153 (2009).

[2] H. Tanaka, *et al.*, Nuclear Phys. B **175**, 280 (2008).

[3] A. Basak, *et al*, DAE Symp. on Nucl. Phys. (Proc.) **65** (2021).

[4] D. Heck, *et al*, FZKA report-6019 ed. FZK Karlsruhe (1998).

[5] N. N. Kalmykov, S. S. Ostapchenko, and A. I. Pavlov, Nucl. Phys. B (Proc. Suppl.) **52**, 17 (1997).

[6] M. Bleicher *et al*, J. Phys. G: Nucl. Part. Phys. **25**, 1859 (1999).

